

Article

Fed-Batch Sucrose Crystallization Model for the B Massecuite Vacuum Pan, Solution by Deterministic and Heuristic Methods

Paulo Eduardo de Morais Gonzales ^{*}, Marcos Antônio de Souza Peloso, Jr., José Eduardo Olivo and Cid Marcos Gonçalves Andrade 

Chemical Engineering Department, State University of Maringá, Colombo Av. 5790, Maringá 87020-900, Brazil; marcospeloso@gmail.com (M.A.d.S.P.J.); jeolivo@uem.br (J.E.O.); cmgandrade@uem.br (C.M.G.A.)

* Correspondence: paulogonzales@outlook.com

Received: 29 January 2020; Accepted: 21 February 2020; Published: 14 September 2020



Abstract: Fed-batch crystallization is a crucial step for sugar production. In order to relate parameters that are difficult to measure (average diameter of the crystals and total mass formed) to other easier to measure parameters (volume, temperature, and concentration), a model was developed for a B massecuite vacuum pan composed of mass and energy balances together with empirical relations that describe the crystal development inside equipment. The generated system of ordinary differential equations (ODE) had eight parameters which were adjusted through minimization of relative differences between the model results and experimental data. It was solved through the function `fmincon`, available in MATLABTM, which is a deterministic and gradient-based optimization method. The objective of this paper is to improve the model obtained and, for this purpose, two metaheuristic functions were used: genetic algorithm and particle swarm. To compare the results, the convergence time of each algorithm was used as well as the resulting quadratic deviation. The particle swarm method was the best option among the three used, presenting a shorter execution time and lower quadratic relative deviation.

Keywords: sucrose; crystallization; fed-batch; metaheuristic method; deterministic method; modeling

1. Introduction

Crystallization is the main process in the sugar industry for the separation and obtaining of sucrose in its commercial form, sugar, and is one of the crucial steps to increase the yield from the plant [1]. Among all steps of sugar production, fed-batch crystallization is the most complex in operational terms since it requires greater care by the plant operators [2].

The industrial sucrose crystallization process consists of three basic equipment: vacuum pan, crystallizer, and centrifuge. In the vacuum pan, sugar crystals form and grow, at a constant temperature, in a fed-batch process. In crystallizers, the crystals grow due to the cooling of the massecuite, which increases supersaturation. The centrifuges separate the crystals formed from the mother liquor which, once exhausted, is called molasses. In this sequence, about half of the sucrose is recovered as sugar crystal. To maximize this recovery, crystallization schemes are used, inserting new sequences of this equipment that are fed by the molasses from the previous step. These sequences can be repeated once (two massecuites scheme), or twice (three massecuites scheme). It is interesting to note that because each sequence of these equipment recovers around half of the crystals, a two massecuite scheme recovers 75% of the sucrose as crystal, while a three massecuite scheme recovers around 87.5%. Because the cost of establishing a three massecuites plant is 50% higher with a mere 12.5% increase in sucrose recovery and most Brazilian industries have an ethanol plant attached that consumes molasses,

the two massecuites scheme is the most widespread in the country [2,3]. Figure 1 shows the flowchart of the two massecuites scheme.

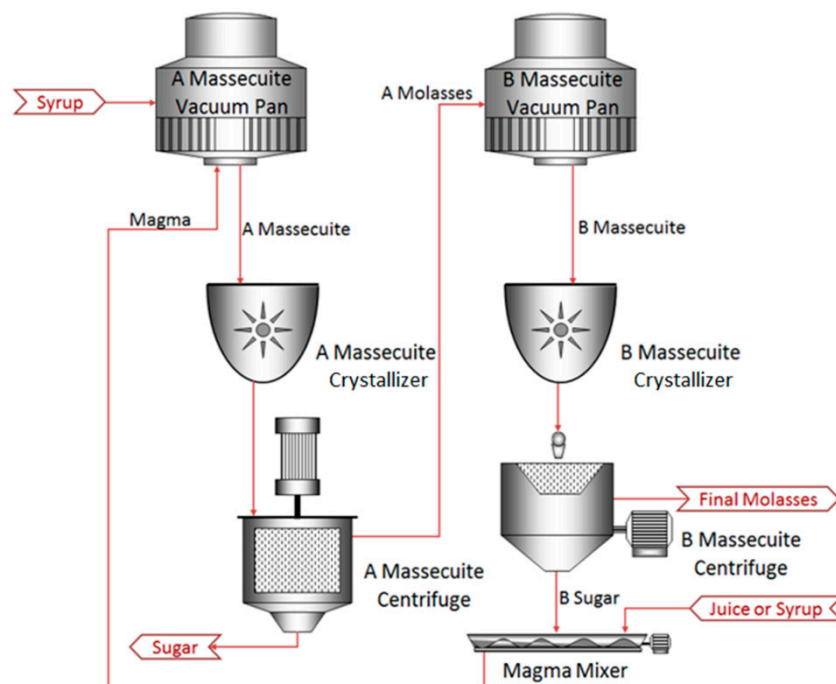


Figure 1. Two massecuites scheme flowchart [4], based on [2].

As Brazil is among the largest sugar producers in the world, the scheme of the two massecuites shown in Figure 1 was the one used in the experiments [3]. As local plants also produce electricity with the steam from the boilers, the massecuite cooling in the crystallizers is not used, which eliminates the need to reheat the massecuite to feed the centrifuges (cooling increases the viscosity of the mother liquor) [3,4]. Thus, the crystallization of sucrose occurs only in vacuum pans, making its study the focus of this work.

The instrumentation of massecuite vacuum pans is a challenge for automation companies due to the high values of the sensors and large amount of equipment to be monitored [5,6]. In order to reduce these costs, two models were developed to relate the mean diameter of the crystals D (4,3) and the total formed crystal mass (FCM)—the data of which are difficult to measure—with the equipment concentration, volume, and temperature; one for A massecuite vacuum pan and the other for B massecuite vacuum pan [7]. Both models were solved through the function *fmincon*, available in MATLAB™, which is a deterministic and gradient-based optimization method [8,9].

With these models, it is possible to develop soft sensors to measure crystal size and quantity in the vacuum pan. It is essential that the program is fast and accurate. Thus, to improve the model obtained for B massecuite vacuum pan, which has eight parameters for adjustment (seven kinetic parameters and a thermodynamic data), two metaheuristic methods were used—genetic algorithm (GA) and particle swarm. To compare the results, the convergence time of each algorithm was used as well as the relative resulting quadratic deviation.

2. Methodology

The equipment used to obtain the experimental data is installed in a São Paulo state sugarcane industry. During the experiment, the volume, concentration, and temperature data of the fluid were recorded by the sensors installed in the equipment. Each batch occurred in two hours, and samples were taken every fifteen minutes through the equipment probe to evaluate both FCM and D (4,3) through a Nikon Eclipse E200-LED Binocular microscope. Figure 2 shows how the crystals look at the

end of the crystallization process in B massecuite vacuum pan and Figure 3 shows the distribution curve of the crystal size at the last point of the first experiment.

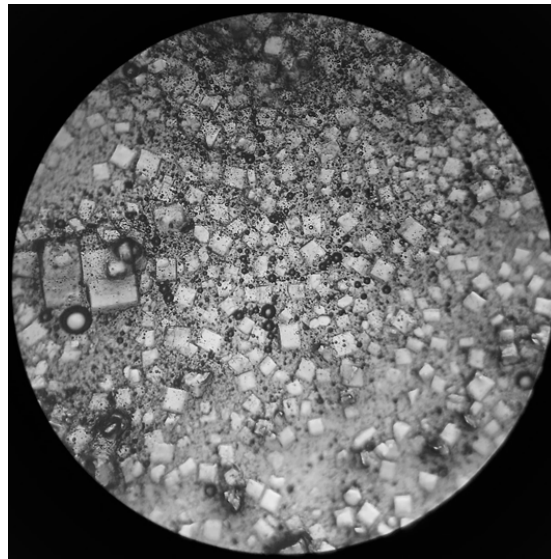


Figure 2. Sucrose crystals at the end of the process.

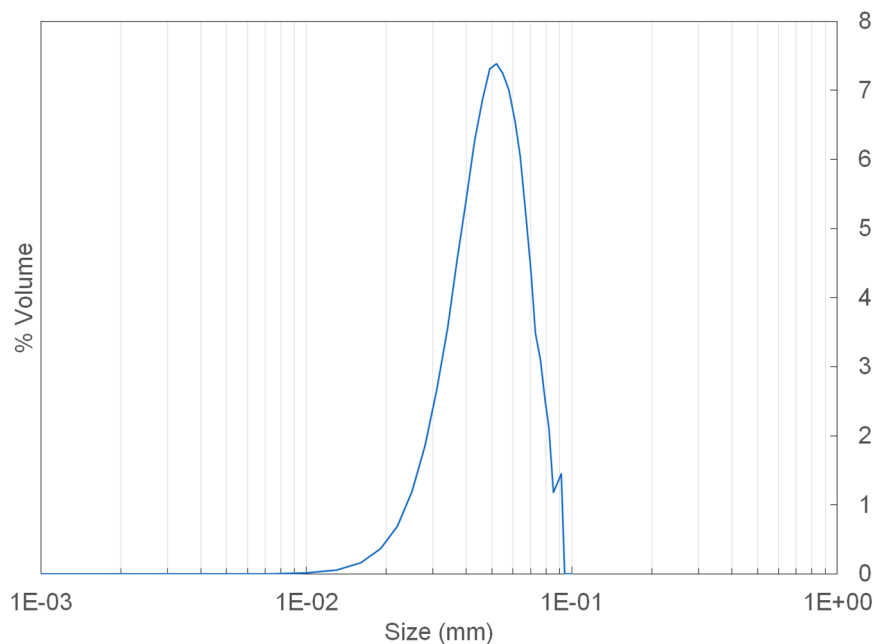


Figure 3. Size distribution curve of the last point of the first experiment.

The mathematical modeling was adapted to a model of a process in pilot scale—batch crystallization with cooling (using evaporation and cooling the solution)—as developed in [10]. The pilot scale process starts with approximately 752 cm³ of syrup, operating for 40 min at 60 °C and is then cooled for 50 min to 40 °C. During its operation, the massecuite volume decreases since it is not fed with syrup and due to evaporation of part of its contents. The B massecuite vacuum pan operation starts with one-third of the equipment volume (10 m³) filled with syrup, occurring for two hours at a constant temperature of 80 °C, receiving a variable flow of A molasses so that the volume of equipment reaches its end capacity (30 m³) in compensating for evaporation of the solvent. The differences between the two processes are summarized in Table 1.

Table 1. Differences between batch crystallization and B massecuite pan.

Characteristic	Batch Crystallizer	B Massecuite Vacuum Pan
Scale	Pilot	Industrial
Feed	Just in beginning	Throughout the process
Crystals initial size	0.0019126 cm	0.030 cm
Equipment's fluid volume	Decreases	Increases
Operation temperature	60 °C, followed by cooling to 42 °C	80 °C throughout the process

The population balance of crystals of the model used in this paper is calculated using the following partial differential equation (PDE) [7,10,11]. This PDE is shown in Equation (1):

$$\frac{\partial(nV)}{\partial t} + \frac{V\partial(Gn)}{\partial L} = V(\alpha(L)) \quad (1)$$

with initial condition

$$n(L, t) = n_0(L, t) \quad t = 0$$

and the boundary condition

$$n(L_0, t) = \frac{B^0}{G_{L=L_0}} \quad (2)$$

$\alpha(L)$ is known as production-reduction term and it groups the rates of birth and destruction of crystals. Applying the method of moments (MOM) in Equation (1), the following system of ordinary differential equations (ODEs), presented in Equations (3) and (4), is obtained [10]:

$$\frac{d\mu_0}{dt} = B^0 \quad (3)$$

$$\frac{d\mu_k}{dt} = kG\mu_{k-1}(1 + \ln(V)) \quad k = 1 \dots 3 \quad (4)$$

where V is the mass volume inside the equipment in cm^3 . The number of moments necessary for the model resolution can tend to infinity, but due to the use of the empirical equation shown below (Equation (5)), the moment μ_3 enters the mass balance, causing the four moments (μ_0 , μ_1 , μ_2 , and μ_3) to be enough to solve the ODE system [12].

B^0 (N° particles/ cm^3 min) and G (cm/min) are the nucleation and growth rates, respectively, that can be modeled by the empirical power equations presented in Equations (5) and (6) [10]:

$$B^0 = K_b S_r^b M_T^j N_r^p \quad (5)$$

$$G = K_g S_r^g N_r^q \quad (6)$$

N_r is the stirrer speed in rpm. The terms K_b (N° part/ $\text{cm}^3 \cdot \text{min} \cdot (\text{g}/\text{cm}^3)^j \cdot (\text{rpm})^p$), b , j , p , K_g ($\text{cm}/\text{min} \cdot (\text{rpm})^q$), g , and q are the kinetic parameters of these equations and were estimated and optimized using the experimental data.

In Equation (5), M_T represents the total mass of crystals and can be obtained using Equation (7):

$$M_T = \rho_c K_v \mu_3(t) \quad (7)$$

where ρ_c is the density of the sucrose in g/cm^3 , and $K_v = \pi/6$ is the characteristic form factor for sugar crystals [10,13].

In Equations (5) and (6), S_r represents the relative supersaturation, and is defined by Equation (8):

$$S_r = \frac{C - C_{sat}}{C_{sat}} \quad (8)$$

where C is the sucrose concentration and C_{sat} is the saturation concentration point, both in g/cm^3 . The mass percentage of sucrose in the saturated solution ($Brix_{sat}$) can be calculated as a function of temperature using Equation (9) [4,7,14].

$$Brix_{sat} = 5.1844 \times 10^{-4} T^2 + 1.3575 \times 10^{-1} T + 64.168 \quad (9)$$

where T is the temperature in $^{\circ}\text{C}$.

The density of a sucrose solution (ρ) can be obtained by Equation (10) (T in $^{\circ}\text{C}$) [7,15]:

$$\rho = \left(1 + Brix \frac{(Brix + 200)}{54000} \right) \times \left(1 - 0.036 \frac{(T - 20)}{(160 - T)} \right). \quad (10)$$

The solution concentration, as well as its saturation concentration, can be obtained by Equation (11):

$$C = \frac{\rho \times Brix}{100}. \quad (11)$$

The mass balance of the process is presented in Equation (12) [7]:

$$m_{sucrose}(t) = C_{mA} V_{mA} + m_{sucrose}^0 \quad (12)$$

where $m_{sucrose}$ and $m_{sucrose}^0$ is the total mass of sucrose (g) in the equipment at time t and 0 , respectively, C_{mA} is the concentration of A-molasses (g/cm^3), and V_{mA} is the accumulated flow of A-molasses added in equipment (cm^3). Equation (13) shows that the total mass of sucrose inside the equipment is partly in solution (CV_S) and partly crystallized ($\rho_c V_c$):

$$m_{sucrose}(t) = C V_S + \rho_c V_c. \quad (13)$$

Equation (14) shows that the volume of the solution (V_S) plus the volume of the crystals (V_c) is equivalent to the volume of massecuite in the equipment (V).

$$V = V_S + V_c \quad (14)$$

Rearranging:

$$V_S = V - V_c. \quad (15)$$

Thus, replacing Equations (13) and (14) in Equation (12):

$$C (V - V_c) + \rho_c V_c = C_{mA} V_{mA} + m_{sucrose}^0, \quad (16)$$

deriving Equation (16) the Equation (17) is obtained:

$$\frac{dC}{dt} (V - V_c) + C \left(\frac{dV}{dt} - \frac{dV_c}{dt} \right) + \rho_c \frac{dV_c}{dt} = C_{mA} \frac{dV_{mA}}{dt}. \quad (17)$$

Substituting V_c for $K_v \mu_3(t)$ and isolating dC/dt leads to Equation (18):

$$\frac{dC}{dt} = \left(\frac{1}{V - \mu_3(t) K_v} \right) \times \left(C_{mA} \frac{dV_{mA}}{dt} + (C - \rho_c) K_v \frac{d\mu_3}{dt} - C \frac{dV}{dt} \right) \quad (18)$$

with initial condition

$$C(0) = C_0. \quad (19)$$

The energy balance of B massecuite vacuum pan is shown in Equation (20) [2]:

$$E(t) = Q - W + F_{in}h_{in} - F_{out}h_{out} \quad (20)$$

where $E(t)$ is the internal energy of the system in J, F_{in} and F_{out} are the mass input and output in g, h_{in} and h_{out} the relative enthalpies in J/g. Replacing the Equation (20) variables with those of the B vacuum pan [7,10]:

$$m_{VC}Cp_{VC}\Delta T_{VC} = Q - W + m_{mA}Cp_{mA}\Delta T_{mA} - m_{ev}H_{ev} - m_c\Delta H_c. \quad (21)$$

The subscripts m_A and VC represent A molasses and mass in vacuum pan, respectively. Deriving Equation (21):

$$m_{VC}Cp_{VC}\frac{dT}{dt} = \dot{Q} - \dot{W} + Cp_{mA}\Delta T_{mA}\frac{dm_{mA}}{dt} - \frac{d(m_{ev}H_{ev})}{dt} - \Delta H_c\frac{dm_c}{dt}. \quad (22)$$

The heat rate can be obtained by Equation (23) [2]:

$$\dot{Q} = U_l A_l (T_j - T). \quad (23)$$

T_j is the temperature of the steam in the equipment's calandria ($^{\circ}\text{C}$), U_l is the global coefficient of thermal exchange ($\text{J}/(^{\circ}\text{C}\cdot\text{min}\cdot\text{cm}^2)$), and A_l is the heat exchanger area (cm^2). The work rate is calculated by Equation (24) [11]:

$$\dot{W} = -\frac{d(PV)}{dt} \quad (24)$$

where P is the absolute pressure in J/cm^3 . Replacing Equations (23) and (24) in Equation (22) and explaining the volumes of A molasses and crystals formed, Equation (25) is obtained:

$$\frac{dT}{dt} = \frac{\frac{d(PV)}{dt} - \frac{d(H_{ev}m_{ev})}{dt} + (\rho CpT)_{mA}\frac{dV_{mA}}{dt} - \Delta H_c \rho_c K_v \frac{d\mu_3}{dt} + U_l A_l (T_j - T)}{(\rho VCp)_{VC}} \quad (25)$$

with initial condition

$$T(0) = T_0. \quad (26)$$

ΔH_c is the crystallization heat in J/g, which can be calculated by means of Equation (27) (T in $^{\circ}\text{C}$) [10,13]:

$$\Delta H_c = -12.2115 - 0.7937T. \quad (27)$$

Also in Equation (25), m_{ev} is the evaporated accumulated mass flow rate and H_{ev} is the vaporization enthalpy in J/g, which can be obtained by Equation (28) (T in $^{\circ}\text{C}$) [16]:

$$H_{ev} = 4.1868 \times (607 - 0.7T). \quad (28)$$

The absolute pressure P , in J/cm^3 , within the equipment can be obtained using the Antoine equation presented in Equation (29) (T in $^{\circ}\text{C}$) [16]:

$$P = 2.21 \times 10^1 e^{(6.53247 - \frac{7173.79}{1.87 + 421.4747})}. \quad (29)$$

The specific heat of sucrose solutions, Cp in $\text{J}/\text{g}\cdot^{\circ}\text{C}$, can be obtained by means of Equation (30) (T in $^{\circ}\text{C}$) [7,15,17]:

$$Cp = p_1 + p_2.Brix + p_3.Brix.T + p_4.T + p_5.T^2. \quad (30)$$

The dynamics of the volume of liquid inside the equipment, V in cm^3 , is described by Equation (31), which is a cubic correlation obtained through the equipment data during the experiment (t in min):

$$V(t) = -1.5896t^3 - 75.299t^2 + 1.9859 \times 10^5t + 10^7. \quad (31)$$

Table 2 presents the parameters used in this modeling:

Table 2. Process parameters to solve the population, mass, and energy balances.

Parameter	Value	Unit
K_v	$\pi/6$	–
A_l	1950000	cm^2
L_0	0.030	cm
p_1	4.12553	$\text{J/g } ^\circ\text{C}$
p_2	−0.024804	$\text{J/g } ^\circ\text{C}$
p_3	0.000067	$\text{J/g } (^\circ\text{C})^2$
p_4	0.0018691	$\text{J/g } (^\circ\text{C})^2$
p_5	−0.000009271	$\text{J/g } (^\circ\text{C})^3$
T_{mA}	80	$^\circ\text{C}$
T_0	80	$^\circ\text{C}$
T_j	131	$^\circ\text{C}$
C_{mA}	1.0085	g/cm^3
C_0	1.0733	g/cm^3
N_r	300	rpm

In Equations (5) and (6), the proposed mathematical model includes seven kinetic parameters (K_b , b , j , p , K_g , g , and q) specific for each batch crystallization operating condition [10]. These values need to be adjusted so that the model provides representative results of this process. The global coefficient of thermal exchange (U_l) was also added in the adjustment [7]. Based on this, it sought to reduce the relative quadratic differences between the experimental data and those obtained by the model, according to Equation (32):

$$\min \sum_{i=1}^n \left(\frac{CSD_{exp,i} - CSD_{model,i}}{CSD_{exp,i}} \right)^2 \quad (32)$$

In the model deterministic solution, the non-linear optimization tool *fmincon*, available in MATLABTM, was used in conjunction with the use of the *ode23s* [7,10]. In this paper Equation (32) was also solved using two metaheuristic tools, one based on the genetic algorithm (*ga*) and the other on the particle swarm (*particleswarm*) [18,19]. The results were obtained with the hardware configuration shown in Table 3:

Table 3. Hardware configuration used in the modeling.

CPU	i7 4770k
RAM	2 × DDR3 1600 MHz-08 GB
HD	240 GB SSD SATA 3

The algorithms were executed in order to record the convergence time and the relative quadratic deviation of the obtained results with the experimental data.

3. Results and Discussion

Table 4 presents the operational data from experiments 1 and 2:

Table 4. Operational data from experiments 1 and 2 (V_{mA} is accumulative).

t (min)	Experiment 1					Experiment 2				
	V_{VC} (m ³)	T (°C)	C (g/cm ³)	S_r	V_{mA} (m ³)	V_{VC} (m ³)	T (°C)	C (g/cm ³)	S_r	V_{mA} (m ³)
0	10.02	78.98	1.072	0.018	0.000	9.87	80.81	1.074	0.003	0.000
5	11.17	80.44	1.079	0.022	1.420	10.64	80.13	1.077	0.021	1.900
10	12.25	80.04	1.079	0.027	2.495	11.74	79.62	1.079	0.035	3.905
15	13.23	80.53	1.084	0.038	3.693	13.28	79.79	1.089	0.063	4.686
20	13.93	79.13	1.085	0.061	4.681	13.77	80.37	1.086	0.047	5.714
25	15.05	80.45	1.088	0.053	6.058	13.83	81.10	1.089	0.046	6.680
30	15.96	79.79	1.090	0.068	7.159	14.80	80.40	1.090	0.059	8.022
35	16.87	80.22	1.091	0.064	8.008	15.91	79.85	1.091	0.072	9.205
40	17.58	79.00	1.093	0.091	9.771	16.86	80.00	1.091	0.070	11.123
45	18.09	80.27	1.094	0.077	11.705	17.74	80.24	1.093	0.071	12.484
50	19.27	78.81	1.094	0.096	13.382	19.43	79.84	1.094	0.083	13.872
55	21.04	80.16	1.094	0.076	14.258	21.03	79.13	1.095	0.096	14.780
60	21.76	80.00	1.095	0.084	16.005	22.67	79.58	1.096	0.092	15.652
65	22.33	80.03	1.098	0.093	17.458	23.88	79.61	1.095	0.088	16.757
70	22.79	80.43	1.096	0.082	18.858	24.20	79.40	1.097	0.100	17.418
75	24.18	79.80	1.098	0.095	20.022	24.85	79.70	1.099	0.102	17.997
80	25.77	79.80	1.101	0.107	21.300	24.81	80.03	1.099	0.095	19.391
85	25.71	80.10	1.102	0.106	22.991	25.82	79.46	1.101	0.112	21.282
90	26.34	80.70	1.104	0.104	24.296	27.40	79.83	1.106	0.125	23.182
95	26.33	79.77	1.108	0.135	25.278	27.65	80.49	1.107	0.119	24.570
100	26.60	79.64	1.111	0.149	26.030	28.42	80.28	1.108	0.127	25.223
105	27.54	79.28	1.113	0.160	27.339	28.89	80.25	1.115	0.154	26.433
110	29.20	80.80	1.118	0.158	28.310	28.80	79.91	1.120	0.180	28.144
115	29.60	80.36	1.126	0.197	29.465	30.12	80.28	1.125	0.194	29.655
120	30.23	80.21	1.134	0.232	30.086	30.87	79.60	1.134	0.241	30.394

In these conditions, the size of formed crystals and their quantity were evaluated, shown in Table 5:

Table 5. B Masecuite crystals experimental data.

t (min)	Experimental 1		Experimental 2	
	D (4,3) (cm)	MCF (ton)	D (4,3) (cm)	MCF (ton)
0	0.029	3.68	0.030	3.83
15	0.034	5.86	0.034	5.86
30	0.034	6.04	0.036	6.95
45	0.038	8.46	0.039	9.07
60	0.044	12.26	0.042	10.98
75	0.044	12.62	0.043	11.53
90	0.047	15.34	0.047	15.34
105	0.053	21.49	0.049	17.80
120	0.054	23.60	0.056	25.40

With known data from Tables 2, 4 and 5, the ODE system was solved using the two meta-heuristic methods to reduce the differences between the results of the model obtained in relation to the two experiments (Equation (32)), thereby, obtaining the unknown parameters—the seven kinetic parameters and global coefficient of thermal change (U_i) of system—presented in Tables 6 and 7 along

with the parameters of deterministic solution. Although they have different values, the order of magnitude remained.

Table 6. Kinetic parameters of crystals nucleation rate.

Solution	K_b ($N^\circ \text{ Part/cm}^3 \cdot \text{min} \cdot (\text{g/cm}^3)^j \cdot (\text{rpm})^p$)	b	j	p
Deterministic	9.91×10^{-3}	8.00×10^{-4}	4.00×10^{-3}	1.16
GA	9.10×10^{-3}	6.00×10^{-4}	3.53×10^{-3}	1.16
Particle Swarm	9.00×10^{-3}	5.11×10^{-4}	7.99×10^{-3}	0.90

Table 7. Kinetic parameters of crystals growth rate and global coefficient of thermal change.

Solution	K_g ($\text{cm/min} \cdot (\text{rpm})^g$)	g	Q	U_l ($\text{J}/(\text{C min cm}^2)$)
Deterministic	1.89×10^{-6}	1.50×10^{-1}	4.55×10^{-1}	0.8745
GA	4.35×10^{-6}	1.51×10^{-1}	3.09×10^{-1}	0.8770
Particle Swarm	3.81×10^{-6}	0.90×10^{-1}	2.89×10^{-1}	0.8720

Table 8 presents the average execution time of each algorithm and the relative quadratic deviation obtained at the end of the execution of the algorithm.

Table 8. Quadratic deviations and the execution time of each algorithm.

Solution	Deviation ²	Time (min)
Deterministic	1.58%	7.12
GA	0.87%	4.27
Particle Swarm	0.77%	2.82

It is noted that the particle swarm method was able to obtain a smaller deviation with a shorter execution time compared to the other methods. The genetic algorithm also performed better than the deterministic method used by the *fmincon* function. It is noteworthy that some point results of the deterministic solution were able to converge in less time than the average of the other methods, but without approaching the deviations obtained by them. This occurs due to the high dependence of the deterministic methods of the initial point, which in most cases leads them to local minimums [20].

In the graphs shown in Figures 4–6, it is possible to verify that all the algorithms made a good adjustment to the data.

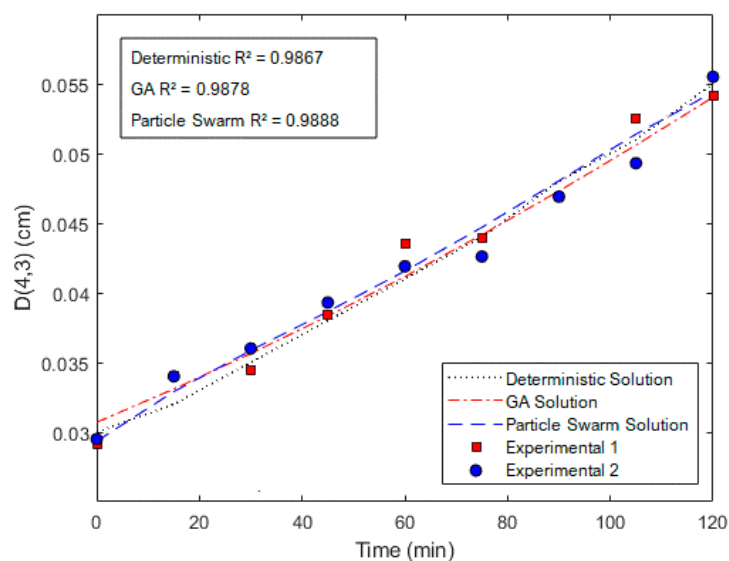


Figure 4. Model results—average crystal size $D(4,3)$.

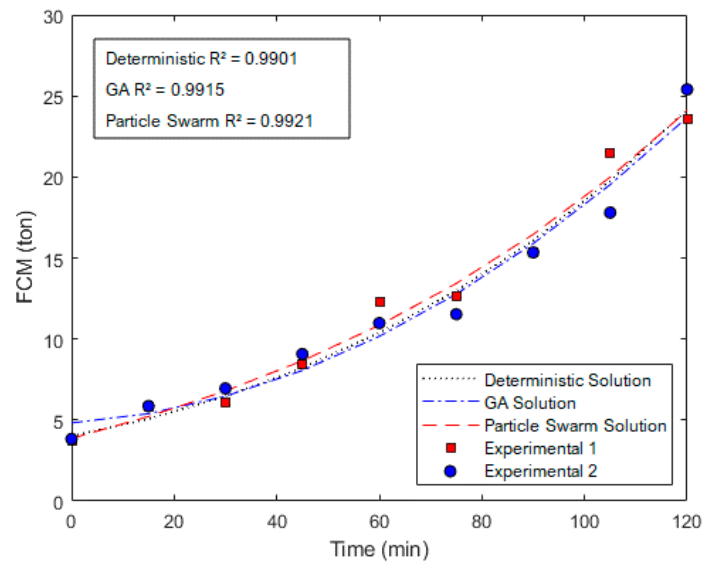


Figure 5. Model results—formed crystal mass (FCM).

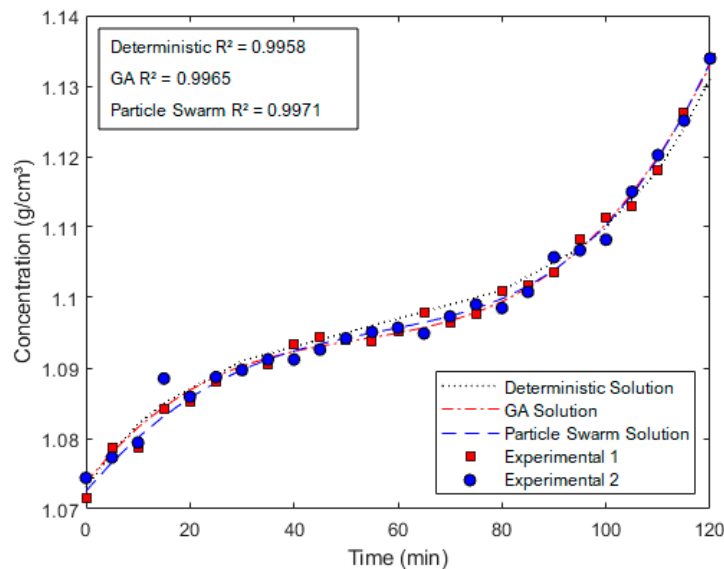


Figure 6. Model results—concentration g/cm^3 .

The correlation coefficient (R^2) values were obtained through multiple linear regressions with both experiments, and followed the behavior of the relative square deviations shown in Table 8. The graphs obtained for the metaheuristic methods were similar to those obtained for the deterministic method [7].

4. Conclusions

This paper has tried to refine a model obtained for B masseuite vacuum pan by implementing metaheuristic methods in the optimization of the kinetic parameters and global coefficient of thermal change. As shown in Table 8 and Figures 4–6, the particle swarm method was the best option among the three used, presenting a shorter execution time, a lower quadratic relative deviation, and higher correlation coefficients (R^2). Nevertheless, when analyzing the data fit, it is noted that all solutions were very close, making the execution time the determining variable for choosing the algorithm to be used, keeping in mind that the development of a soft sensor to measure the size of crystals and their quantity in the vacuum pan is the target of this work. The solution through the deterministic method was highly influenced by the initial point, as expected. As a next step to this work, the refinement of

the model of the operation for A masseuite vacuum pan can be carried out, as well as the use of other functions for comparison.

Author Contributions: Conceptualization, P.E.d.M.G.; methodology, P.E.d.M.G.; software, P.E.d.M.G.; validation, P.E.d.M.G., M.A.d.S.P.J. and J.E.O.; formal analysis, P.E.d.M.G.; investigation, P.E.d.M.G. and M.A.d.S.P.J.; resources, P.E.d.M.G., M.A.d.S.P.J. and J.E.O.; data curation, P.E.d.M.G.; writing—original draft preparation, P.E.d.M.G.; writing—review and editing, P.E.d.M.G. and M.A.d.S.P.J.; visualization, P.E.d.M.G. and C.M.G.A.; supervision, C.M.G.A.; project administration, J.E.O. and C.M.G.A.; funding acquisition, M.A.d.S.P.J. and C.M.G.A. All authors have read and agreed to the published version of the manuscript.

Funding: This research was funded by National Council for Scientific and Technological Development (CNPq) and by Coordination for the Improvement of Higher Education Personnel (CAPES).

Acknowledgments: The authors would like to thank the National Council for Scientific and Technological Development (CNPq) and the Coordination for the Improvement of Higher Education Personnel (CAPES) for financial support.

Conflicts of Interest: The authors declare no conflict of interest.

References

1. Chianese, A.; Kramer, H.J.M. *Industrial Crystallization Process. Monitoring and Control*, 1st ed.; Wiley-VCH: Weinheim, Germany, 2012.
2. Hugot, E. *Handbook of Cane Sugar Engineering*, 3rd ed.; Elsevier Pub. Co: New York, NY, USA, 1986.
3. Gonzales, P.E.d.M.; Fermo, I.R.; Almeida, E.L.; Andrade, C.M.G. Industrial Processes of Sucrose Crystallization: A Brief Review. In Proceedings of the 10th International Conference on Sustainable Energy and Environmental Protection: Mechanical Engineering, Bled, Slovenia, 27–30 June 2017; pp. 29–40. [\[CrossRef\]](#)
4. Bubník, Z.; Henke, S.; Hinková, A.; Pour, V. Database of the Properties of Sucrose, Sucrose Solution and Food. *J. Food Eng.* **2006**, *77*, 399–405. [\[CrossRef\]](#)
5. Meng, Y.; Lan, Q.; Qin, J.; Yu, S.; Pang, H.; Zheng, K. Data-Driven Soft Sensor Modeling Based on Twin Support Vector Regression for Cane Sugar Crystallization. *J. Food Eng.* **2019**, *241*, 159–165. [\[CrossRef\]](#)
6. Ferreira, A.; Faria, N.; Rocha, F.; Teixeira, J.A. Using an Online Image Analysis Technique to Characterize Sucrose Crystal Morphology during a Crystallization Run. *Ind. Eng. Chem. Res.* **2011**, *50*, 6990–7002. [\[CrossRef\]](#)
7. Gonzales, P.E.d.M. *Modelagem Dinâmica Da Cristalização Em Batelada Alimentada Da Sacarose No Processo de Duas Massas*; Universidade Estadual de Maringá: Maringá, Brazil, 2019.
8. Regis, R.G.; Shoemaker, C.A. A Quasi-Multistart Framework for Global Optimization of Expensive Functions Using Response Surface Models. *J. Glob. Optim.* **2013**, *56*, 1719–1753. [\[CrossRef\]](#)
9. Byrd, R.H.; Gilbert, J.C.; Nocedal, J. A Trust Region Method Based on Interior Point Techniques for Nonlinear Programming. *Math Programs* **2000**, *89*, 149–185. [\[CrossRef\]](#)
10. Bolaños-Reynoso, E.; Sánchez-Sánchez, K.B.; Urrea-García, G.R.; Ricardez-Sandoval, L. Dynamic Modeling and Optimization of Batch Crystallization of Sugar Cane under Uncertainty. *Ind. Eng. Chem. Res.* **2014**, *53*, 13180–13194. [\[CrossRef\]](#)
11. Mersmann, A. *Crystallization Technology Handbook*; CRC Press: Boca Raton, FL, USA, 2001.
12. Choong, K.L.; Smith, R. Novel Strategies for Optimization of Batch, Semi-Batch and Heating/Cooling Evaporative Crystallization. *Chem. Eng. Sci.* **2004**, *59*, 329–343. [\[CrossRef\]](#)
13. Hicks, T.G.; Chohey, N.P. *Handbook of Chemical Engineering Calculations*; McGraw-Hill: New York, NY, USA, 2012.
14. Browne, C. *A Handbook of Sugar Analysis: A Practical and Descriptive Treatise for Use in Research, Technical and Control Laboratories*; J. Wiley & Sons: Hoboken, NJ, USA, 1912.
15. Peacock, S. Predicting Physical Properties of Factory Juices and Syrups. *Int. Sugar J.* **1995**, *97*, 571–577.
16. Perry, R.H.; Green, D.W. *Perry's Chemical Engineers' Handbook*; McGraw-Hill: New York, NY, USA, 2008.
17. Bubnik, Z. *Sugar Technologists Manual: Chemical and Physical Data for Sugar Manufacturers and Users*; Albert Bartens: New York, NY, USA, 1995.

18. Conn, A.R.; Gould, N.I.M.; Toint, P.L. A Globally Convergent Augmented Lagrangian Algorithm for Optimization with General Constraints and Simple Bounds. *SIAM J. Numer. Anal.* **1991**, *28*, 545–572. [[CrossRef](#)]
19. Poli, R.; Kennedy, J.; Blackwell, T. Particle Swarm Optimization. *Swarm Intell.* **2007**, *1*, 33–57. [[CrossRef](#)]
20. Ridder, B.J.; Majumder, A.; Nagy, Z.K. Population Balance Model-Based Multiobjective Optimization of a Multisegment Multiaddition (MSMA) Continuous Plug-Flow Antisolvent Crystallizer. *Ind. Eng. Chem. Res.* **2014**, *53*, 4387–4397. [[CrossRef](#)]



© 2020 by the authors. Licensee MDPI, Basel, Switzerland. This article is an open access article distributed under the terms and conditions of the Creative Commons Attribution (CC BY) license (<http://creativecommons.org/licenses/by/4.0/>).